RECTIFICATION AND GEOCODING OF SAR IMAGERY

R. Kwok and J.C. Curlander

Jet Propulsion Laboratory
California Institute of Technology
4800 Oak Grove Drive, Pasadena, California 91109

RESUME

Un post processeur qui rectifie et géocode automatique les images SAR a été develope. Ce procédé accepte une image sortant directement due correlateur SAR operationel et produit une image rectifiée at géocodée. Rectifée indique que les distorsions géomètriques inherentes au radar décentré (side-looking) ont été corrigées. Géocodée refere à l'opération qui consiste à projecter et ajuster sur un maillage cartographique. L'image obtenue a donc l'orientation spécifiée par let maillage. Les images resultantes presentent des erreurs absolues de positionnement de moins de 50m et une distorsion de moins de 0.1% relative aux variations locales des géoides.

ABSTRACT

An automated post-processor for rectification and geocoding of SAR (Synthetic Aperture Radar) imagery has been developed. The processor uses as input the raw image output of the operational SAR correlator and produces as output geometrically rectified and geocoded SAR images. Rectification is the removal of geometric distortions that are inherent in a side-looking radar image. Geocoding is the mapping of the SAR image pixels into a cartographic grid and alignment of the output image pixels with the coordinate frame defined by the map grid. The rectification and geocoding processes have been tested with SEASAT and SIR-B images. The output products have absolute location uncertainty of less than 50m and relative distortion (scale factor and skew) of less than 0.1% relative to local variations from the assumed geoid.

Introduction

A side-looking radar is capable of measuring only absolute distance and angle from sensor to target. The result is an image that in near range appears compressed with respect to far range. Furthermore, the terrain induces additional local distortions such as radar foreshortening and layover. Compounding the cross-track or range distortions is the fact that spaceborne imagery also suffers from azimuth distortion due to rotation of the Earth. During processing of the radar data, errors in tracking the Doppler centroid produces along-track translation in the image pixels. These inherent geometric distortions in the radar imagery have been a limiting factor in the interpretation and geoscientific application of data products. Traditionally, these geometric distortions have been corrected by manually located tiepoints and the distortions removed by image resampling.

This paper describes a post-processor designed to interface with the output of the SAR image correlator. It has the capability to produce geocoded image products on a routine basis without operator intervention. The geocoded image products are rectified imagery projected onto a prespecified map grid. The procedures to determine the geolocation of SAR image pixels and to resample the imagery to a geocoded format are described here. The processor's capability to use elevation information to rectify terrain-induced local distortions in side-looking radar imagery is outlined. Finally, the utility of geocoded and terrain-rectified image products are illustrated by mosaics of geocoded images and perspective views of SAR images.

Overview of Rectification and Geocoding

a. Location of SAR Pixels

Precision rectification and geocoding of SAR imagery are dependent on the accurate location of the image pixels on the Earth. A procedure for location determination of these pixels has been previously described (1,2). It utilizes the sensor platform location; a geoid model; the parameters of the data collection system; and the SAR processing parameters. Briefly, it is based on the simultaneous solution of three equations describing the Earth shape and the unique Doppler and range associated with each pixel. To determine the geocentric location of a pixel, an iterative process first intersects the range vector with the geoid to determine a nominal terget location and Doppler. The range vector is then squinted to intersect the appropriate iso-Doppler line given by the target Doppler while maintaining the correct sensor-to-target range. This operation is repeated until the Doppler converges to an expected value.

b. Image Resampling

The foregoing procedure provides the spatial location of a slant range image pixel on the geoid. These geocentric locations are then easily mapped onto the desired cartographic projections by using the appropriate transformations. Geocoding also involves the rotation of the rectified image which is in a range-azimuth representation into a reference frame defined by map grid. Since the spatial transformations generated by the model are separable into two principal dimensions (range and azimuth), the slant range images are resampled and rotated into the output grid by three sequential one-dimensional resampling passes over the slant range image and the two intermediate images. The slant range image is rectified in azimuth during the first resampling pass. The intermediate image generated during the first pass is rectified in range and sheared in azimuth during the second pass. The third pass is a final image shear of the second intermediate image into the map grid. The image shears in the second and third passes are for rotation of the rectified image into the map grid. The details of the resampling procedure can be found in (3).

c. Rectification of Terrain-induced Distortions

In a geocoded image, all targets are projected onto a smooth Earth geoid. Any deviation of the target elevation from the geoid model results in

local distortions in the radar imagery known as foreshortening or layover (4). Radar foreshortening is the effect of imaged terrain surfaces sloping towards the radar appearing shortened relative to those sloping away from the radar. Radar layover is an extreme case of foreshortening when the slope of the terrain is greater than the angle of the incident signal. The range displacement of a target at an elevation h in a slant range image is given by,

$$\text{range displacement} = R_t(h) - R_t(0)$$

where Rt(h) is the actual range to the target with an elevation of h and Rt (C) is the slant range distance to the target orthogonally projected onto the geoid. Effectively, these local terrain-induced distortions can be rectified if a digital elevation model (DEM) exists for the area of interest and the radar image is spatially co-registered with the DEM.

The residual registration error between the DEM (registered to a map grid) and the radar imagery is mostly due to along and across track uncertainties in the sensor platform position. In our technique, these translational residuals are removed with the location of two to three tiepoints within the image frame (5). A procedure has also been developed for automatic tiepoint location. It is based on the registration of simulated radar maps (generated from radar imaging geometry and DEMs) to actual SAR imagery.

Procedure Implementation

The post-processor is configured around a SEL 32/77 minicomputer with a FPS-120B array processor, three 300 MByte disks and 32 MBytes of associated RAM with interfaces to SEL and AP.

Figure 1 shows a dataflow diagram of the implementation of the rectification and geocoding processes. The processor uses as input the raw slant range image generated by the SAR correlator. Initially, the transformation map is generated by the procedure described in the preceding section, it gives the spatial relationship between the range-azimuth pixel coordinates and the cartographic coordinates. The spatial resampling locations of the SAR image pixels onto the cartographic grid are computed from this map. The slant range image is then resampled into the output products by three sequential one-dimensional resampling passes.

For terrain rectification, an additional step for penerating a distortion map which contains the pixel adjustments necessary to account for the range displacement of each target is inserted. These adjustments are combined with the resampling locations (which was generated for a smooth geoid) to produce the correct range resampling locations during the second resampling pass.

Results

a. Location Accuracy

The geodetic location error of image targets was computed by comparing the predicted location of targets on the image and the same features on USGS maps. The location errors due to elevation of the tiepoints were removed before comparisons were made with the map. Typical location errors are on the order of several resolution cells which is expected from SEASAT ephemeris uncertainty and nominal system errors.

b. Examples of Geocoded, Terrain-rectified Images, Mosaics and Perspective Views

Figure 2 shows a geocoded SEASAT image of Ascension Bay projected onto a UTM grid. Figure 3 contains three images: a geocoded SEASAT image, the DEM of the corresponding area and the geocoded image after the rectification of the terrain-induced distortions.

Another advantage of geocoded images is the ease with which these images can be mosaicked together if they have been cast into identical map projections. A mosaic of nine SEASAT frames of the Yukon River area in central Alaska is shown in Figure 4. The radiometric disparities at the seams have been cosmetically smoothed by a technique known as feathering.

Perspective views of SAR images can be generated from the terrain-rectified images which have been registered to DEMs. Figure 5 shows a perspective view of the same area during an ascending and descending SEASAT imaging pass.

Concluding Remarks

The operational post-processor described herein represents a powerful tool for enhancing the geometric quality and interpretability of SAR products. The format of the output products provides for ease of registration of imagery with high relief and with other data sets thus facilitating multitemporal, multi-sensor image analysis. The procedures described above can be easily adapted to process SAR image data to generate geocoded products and mosaics with a high degree of geometric accuracy. These algorithms have been incorporated into the operational processing system that supports the SIR-B user community. In addition, this algorithm is being adopted for processing of SAR data from the European Remote Sensor (ERS-1) at the Alaska SAR facility.

Acknowledgments

The research described in this paper was performed at the Jet Propulsion Laboratory, California Institute of Technology, under contract with the National Aeronautics and Space Administration.

References

(1) Curlander, J.C. 1982, Location of Spaceborne SAR Imagery, IEEE Trans. Geosci. Remote Sensing, Vol. GE-20, 359.

(2) Curlander, J.C. 1984, Utilization of Spaceborne SAR Data for Mapping, IEEE Trans. Geosci. Remote Sensing, Vol. GE-22, 106.

(3) Curlander, J.C., R. Kwok and S.S. Pang, 1987, A Post-processing System for the Automated Rectification and Registration of Spaceborne SAR imagery. To be published in Int. J. of Remote Sensing.

(4) Lewis, A.J. and H.C. MacDonald, 1970. Interpretive and Mosaicking Problems of SLAR imagery. Remote Sensing of Environment, 1, 23.

(5) Kwok, R., J.C. Curlander and S.S. Pang, Rectification of Terrain-Induced Distortions in Radar Imagery. To be published in Photogrammetric Engineering and Remote Sensing.

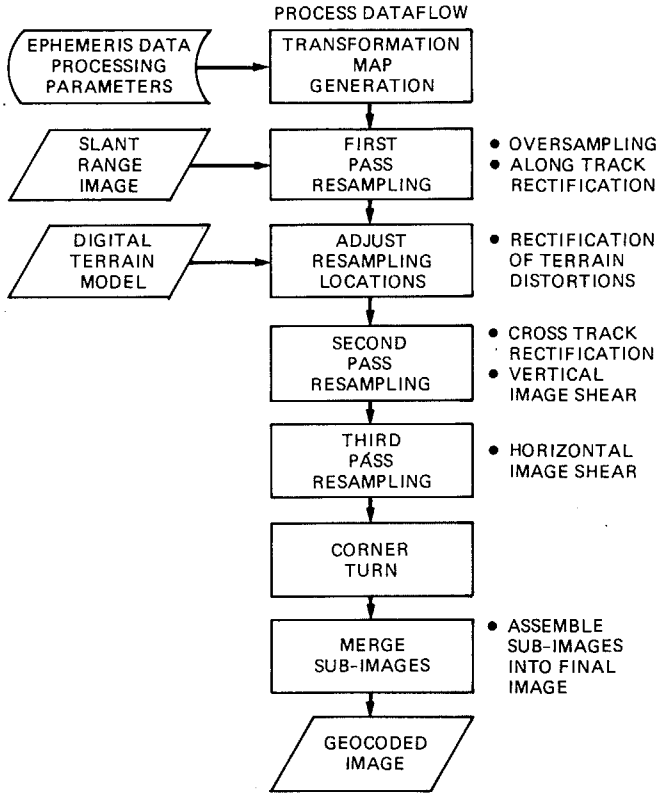

Figure 1. Data Flow of Rectification Process

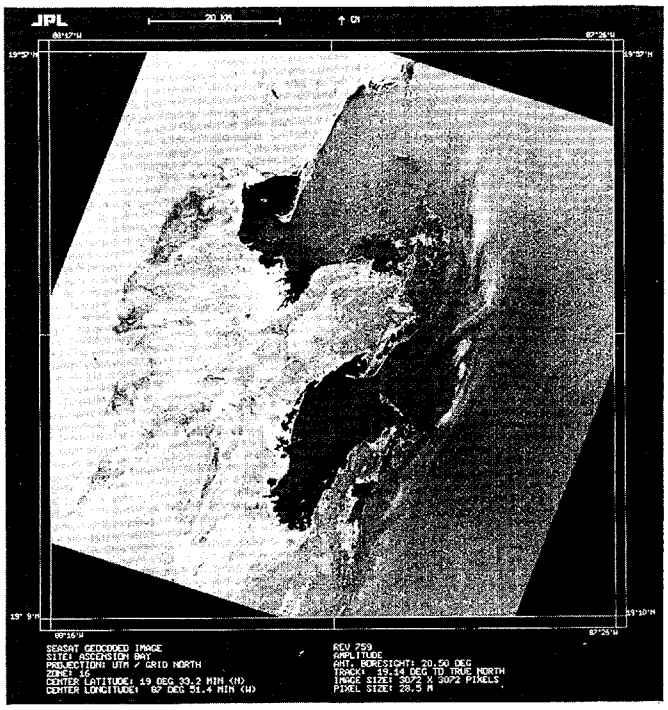

Figure 2. Geocoded SEASAT Image of Ascension Bay (UTM Projection)

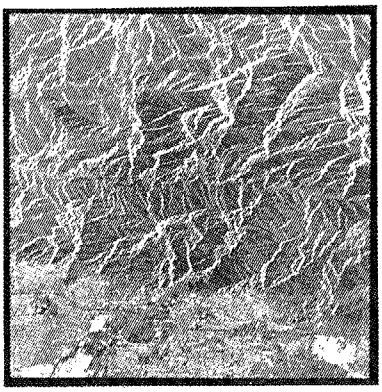

GEOCODED IMAGE

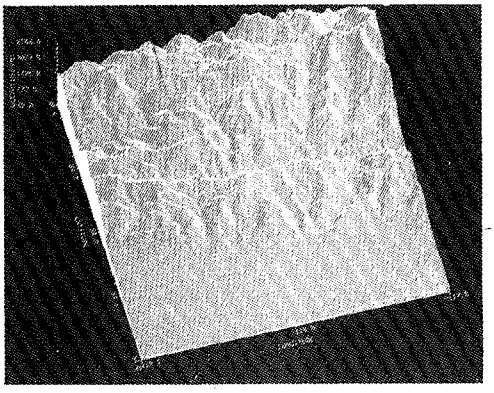

DIGITAL ELEVATION MAP

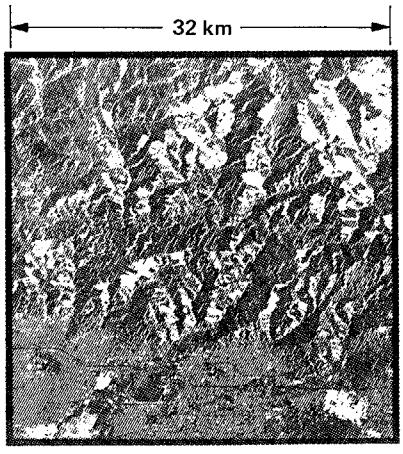

GEOCODED WITH TERRAIN CORRECTION

Figure 3. Rectification of Terrain-Induced Distortions With Digital Elevation Model

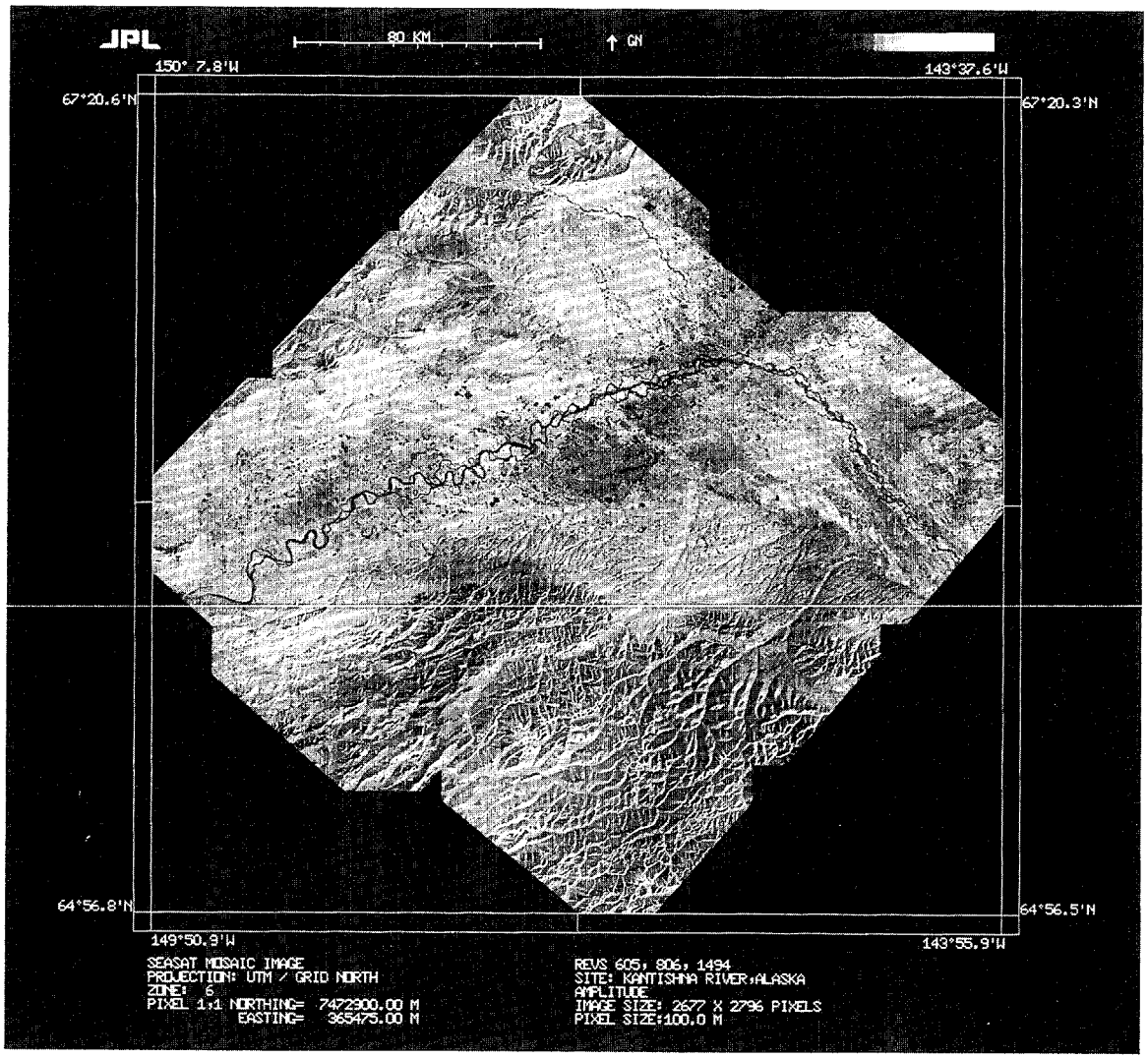

Figure 4. Mosaic of Nine Geocoded SEASAT Image Frames of the Yukon River Area in Central Alaska

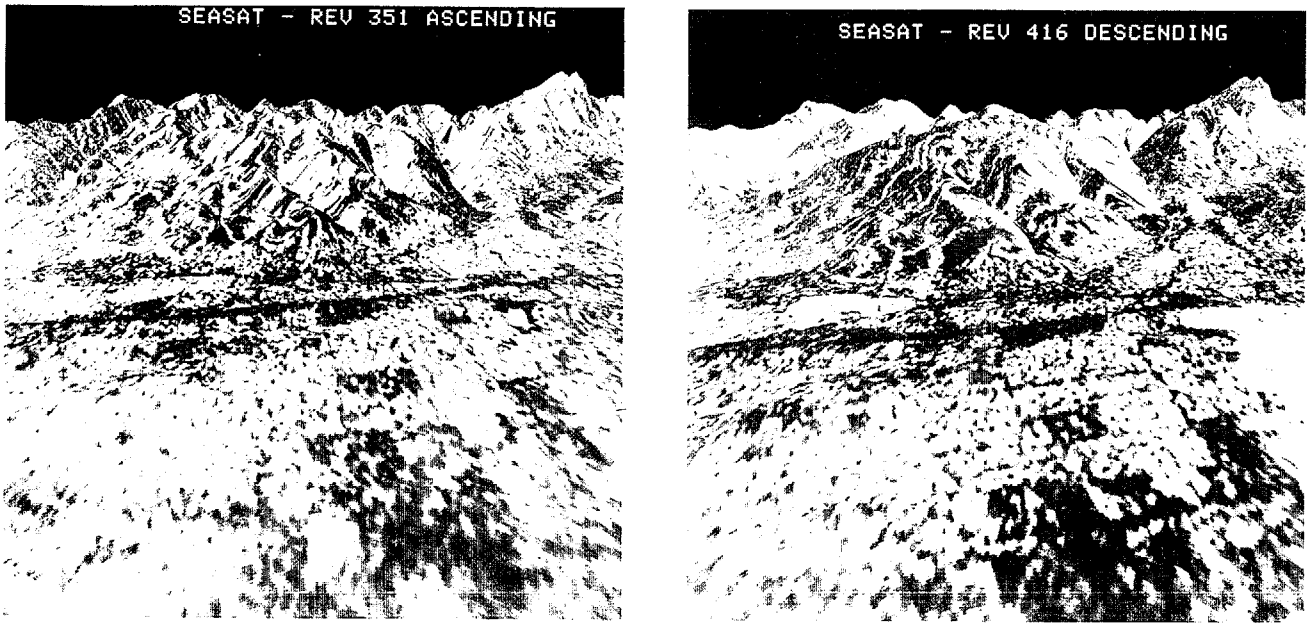

Figure 5. Perspective Projection of Ascending and Descending Imaging Passes Over the Same Area Near the Foothills of Los Angeles